Biophysical Journal, Volume 99

Supporting Material

SANS investigation of the photosynthetic machinery of *Chloroflexus aurantiacus*

Kuo-Hsiang Tang, Volker S. Urban, Jianzhong Wen, Yueyong Xin, Robert E. Blankenship*

Supporting Information

SANS investigation of the photosynthetic machinery of *Chloroflexus aurantiacus*

Kuo-Hsiang Tang, Volker S. Urban, Jianzhong Wen, Yueyong Xin, Robert E. Blankenship*

Data analysis and modeling. The angular (q) dependence of the scattering intensity, $I(q)$, can be generally expressed as follows.

$$I(q) = n\Delta\rho^2 V^2 P(q) S(q)$$

where n is the number density of particles, V is the volume of the particle, $\Delta\rho$ is the difference between the scattering length densities (ρ) of the particle and the solvent (i.e. the contrast factor), $P(q)$ is the form or shape factor that gives information on particle size and shape, and $S(q)$ is the structure factor that describes intermolecular correlations between scattering particles; for dilute solutions $S(q)$ approaches unity. Furthermore, the normalized form factor $P(q)$ as defined above approaches unity as q approaches zero. For small q and absence of inter-particle interference ($S(q) = 1$) several approximations have been derived that allow extraction of particle size in terms of the average radius of gyration (R_g). In analogy to the mechanics of rotating bodies, the radius of gyration (R_g) is defined in SANS as the root-mean-squared distance of all the atoms weighted with their respective neutron scattering length to the center of the scattering length distribution. Such approximations also allow extrapolation to $q = 0$ and therefore determination of the product of q-independent factors in the above equation, which is commonly called forward scattering intensity $I(0)$, and from which e.g. the particle volume can be calculated if the scattering data is calibrated to absolute scale and if the other factors are known. The Guinier approximation, $I(q) = I(0)\exp(-q^2R_g^2/3)$ with R_g x $q_{max} \leq 1.0$, is widely used for analysis of compact particles (1-4), was also employed in this study. Additionally, the cross-sectional radius (R_c) was estimated using the modified Guinier approximation, q x $I(q) = I(0)\exp(-q^2R_c^2/2)$ with R_c x $q_{max} \leq 1.1$, for rod (or cylinder)-like elongated particles (5). Another modified equation, q^2 x $I(q) = I(0)\exp(-q^2R_t^2)$, where $R_t = 12/T$ and T is the thickness of the plates, was used for fitting lamellar (or platelet)-shape particles.

Additionally, R_g, particle distance distribution function ($P(r)$) and the longest distance within the particle (D_{max}) were obtained using the indirect Fourier transform (IFT) method in the program GNOM (6). The R_g determined by the IFT program ($R_g = \frac{\int_0^{D\,max} r^2 p(r)dr}{2\int_0^{Dmax} p(r)dr}$) makes use of the entire scattering curve and is less sensitive to intermolecular interactions. The predicted SANS parameters and scattering profiles calculated from crystal structures for the B880 light-harvesting complex I (LH1) and RC of *Rps. palustris* (PDB ID 1PYH) (7), the RC of *Rb. sphaeroides* (PDB ID 1AIJ) (8), and the LH2 of *Rps. acidophila* (PDB ID 1NKZ) (9) were obtained by the program CRYSON (10). Reconstitution of low-resolution models for the B808-866 complex and RC of *Cfx. aurantiacus* from data collected for B808-866-βOG mixtures in 17% D_2O (the contrast point for βOG) and RC-LDAO mixtures in 5% D_2O (the contrast point for LDAO), respectively, was generated using the modeling program DAMMIN (11). Fifteen runs of DAMMIN were performed and the average structure was optimized and determined by the program DAMAVER (12). All of the *ab initio* models presented in this report were constructed without symmetrical constraint being applied in the modeling program. The program SUPCOMB (13) was used to superimpose the reconstructed model and the atomic resolution structure.

Hydrodynamic diameter size measurement. The hydrodynamic size of particle dispersion were characterized with a ZetaSizer Nano ZS (Malvern Instruments Inc, UK) using dynamic light scattering (DLS). To appropriately compare to the results acquired via SANS, DLS measurements were performed at 24-25 ^oC. The average hydrodynamic diameter ($d(H)$) is

obtained from the following equation: $d(\mathrm{H}) = k\mathrm{T}/3\pi\eta d_o$, where k is the Boltzmann constant, T is the absolute temperature, η is the viscosity of the solution, and d_o is the translational diffusion coefficient (i.e. the velocity of the Brownian motion) of the particles.

Table S1. The size determination of free βOG and B808-866-βOG mixtures estimated by SANS and DLS (*d*(H), hydrodynamic diameter)

Samples	R_g (SANS)	D_{max} (SANS)	*d*(H) (via DLS)	Reported data
0.8% βOG in 100% D_2O	22 ± 2 Å	50 ± 5 Å	50 ± 10 Å	*d*(H), 45-60 Å (ref. (14) in Supporting Information) and R_g, 30 ± 3 Å (with 1.6% βOG; ref. (15) in Supporting Information)
B808-866-βOG (100% D_2O)	54 ± 1 Å	155 ± 5 Å	140 ± 10 Å	

References in Supporting Informaiton:

1. Guinier, A., and G. Fournet. 1955. Small-Angle Scattering of X-Rays:John Wiley & Sons: London, UK.
2. Tang, K. H., M. Niebuhr, C. S. Tung, H. C. Chan, C. C. Chou, and M. D. Tsai. 2008. Mismatched dNTP incorporation by DNA polymerase beta does not proceed via globally different conformational pathways. Nucleic Acids Res 36:2948-2957.
3. Tang, K. H., M. Niebuhr, A. Aulabaugh, and M. D. Tsai. 2008. Solution structures of 2 : 1 and 1 : 1 DNA polymerase-DNA complexes probed by ultracentrifugation and small-angle X-ray scattering. Nucleic Acids Res 36:849-860.
4. Tang, K. H., H. Guo, W. Yi, M. D. Tsai, and P. G. Wang. 2007. Investigation of the conformational states of Wzz and the Wzz.O-antigen complex under near-physiological conditions. Biochemistry 46:11744-11752.
5. Schurtenberger, P., R. Scartazzini, L. J. Magid, M. E. Leser, and P. L. Luisi. 1990. Structural and dynamic properties of polymer-like reverse micelles. J Phys Chem 94: 3695-3701.
6. Semenyuk, A. V., and D. I. Svergun. 1991. Gnom - a program package for small-angle scattering data processing. J Appl Cryst 24:537-540.
7. Roszak, A. W., T. D. Howard, J. Southall, A. T. Gardiner, C. J. Law, N. W. Isaacs, and R. J. Cogdell. 2003. Crystal structure of the RC-LH1 core complex from *Rhodopseudomonas palustris*. Science 302:1969-1972.
8. Stowell, M. H., T. M. McPhillips, D. C. Rees, S. M. Soltis, E. Abresch, and G. Feher. 1997. Light-induced structural changes in photosynthetic reaction center: implications for mechanism of electron-proton transfer. Science 276:812-816.
9. Papiz, M. Z., S. M. Prince, T. Howard, R. J. Cogdell, and N. W. Isaacs. 2003. The structure and thermal motion of the B800-850 LH2 complex from *Rps.acidophila* at 2.0A resolution and 100K: new structural features and functionally relevant motions. J Mol Biol 326:1523-1538.
10. Svergun, D. I., S. Richard, M. H. Koch, Z. Sayers, S. Kuprin, and G. Zaccai. 1998. Protein hydration in solution: experimental observation by x-ray and neutron scattering. Proc Natl Acad Sci U S A 95:2267-2272.
11. Svergun, D. I. 1999. Restoring low resolution structure of biological macromolecules from solution scattering using simulated annealing. Biophys J 76:2879-2886.
12. Volkov, V. V., and D. I. Svergun. 2003. Uniqueness of ab initio shape determination in small-angle scattering. J Appl Cryst 36:860-864.
13. Kozin, M. B., and D. I. Svergun. 2001. Automated matching of high- and low-resolution structural models. J Appl Cryst 34:33-41.
14. Lorber, B., J. B. Bishop, and L. J. DeLucas. 1990. Purification of octyl beta-D-glucopyranoside and re-estimation of its micellar size. Biochim Biophys Acta 1023:254-265.
15. Lipfert, J., L. Columbus, V. B. Chu, S. A. Lesley, and S. Doniach. 2007. Size and shape of detergent micelles determined by small-angle X-ray scattering. J Phys Chem B 111:12427-12438.

Figure S1. The particle size distribution of free βOG micelles and B808-866-βOG mixtures in 100% D_2O buffer acquired by dynamic light scattering (DLS) measurements. The experiments were performed at 25 °C with 0.8% (w/v) βOG included in the samples.

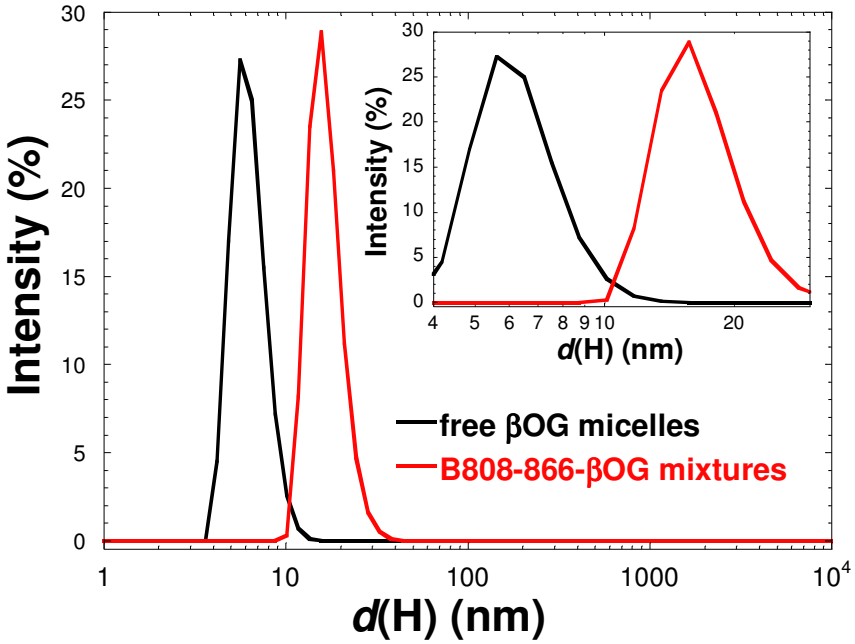

Figure S2. SANS for RC-LDAO mixtures of *Cfx. aurantiacus*. The SANS data for RC-LDAO mixtures in 5, 40 and 100% D_2O (A), the Guinier fit for RC-LDAO mixtures in different concentration of D_2O (B), the *P*(r) profile for RC-LDAO mixtures in 100% (black curve) and 40% D_2O (blue curve) (C), and the normalized *P*(r) profile for RC-LDAO mixtures of *Cfx. aurantiacus* (red curve) and *Rb. sphaeroides* (black curve) in 100% D_2O (D).

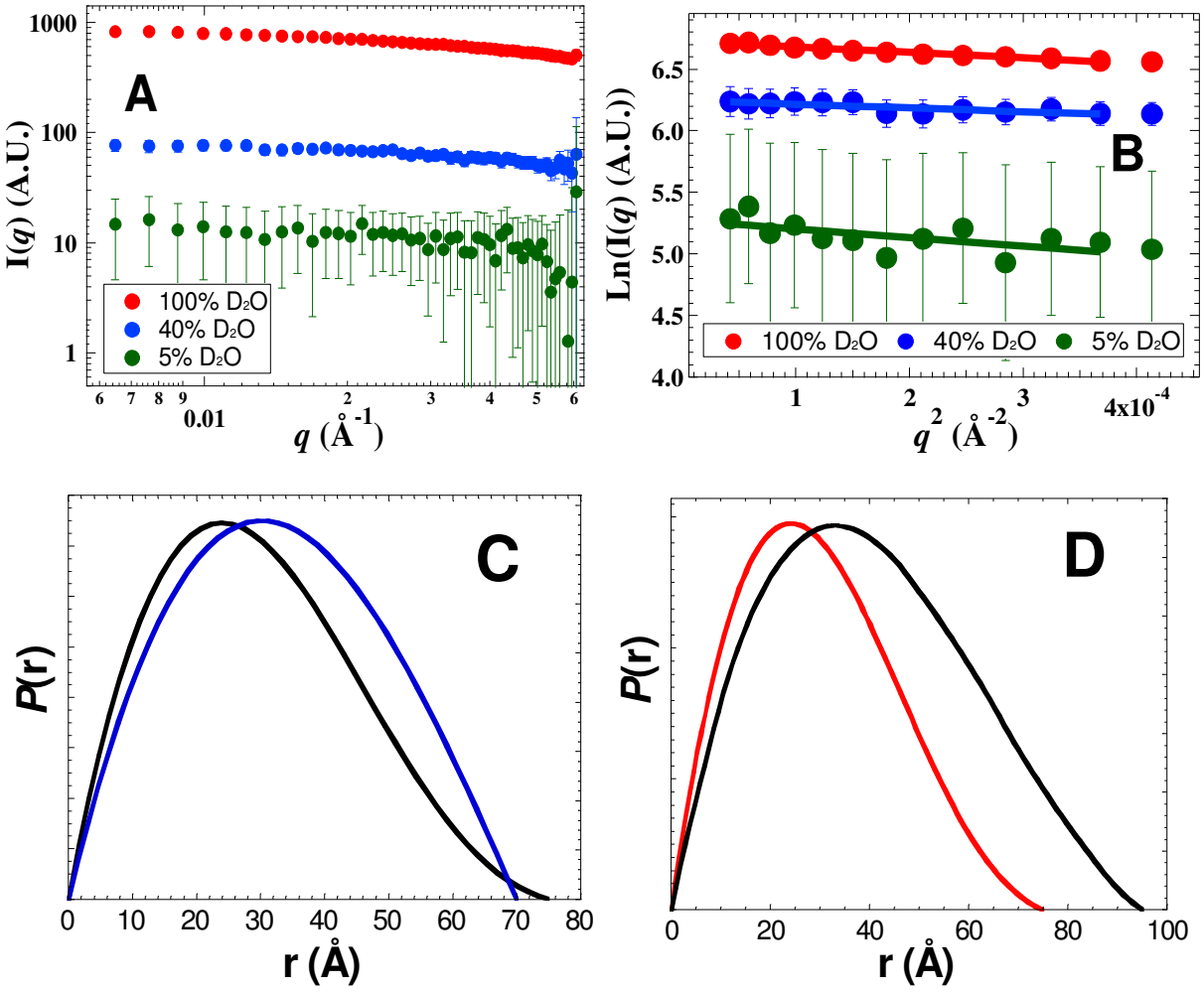

Figure S3. The modified Guinier approximation and the radius of cross section (R_c) of the chlorosome in different concentration of D_2O

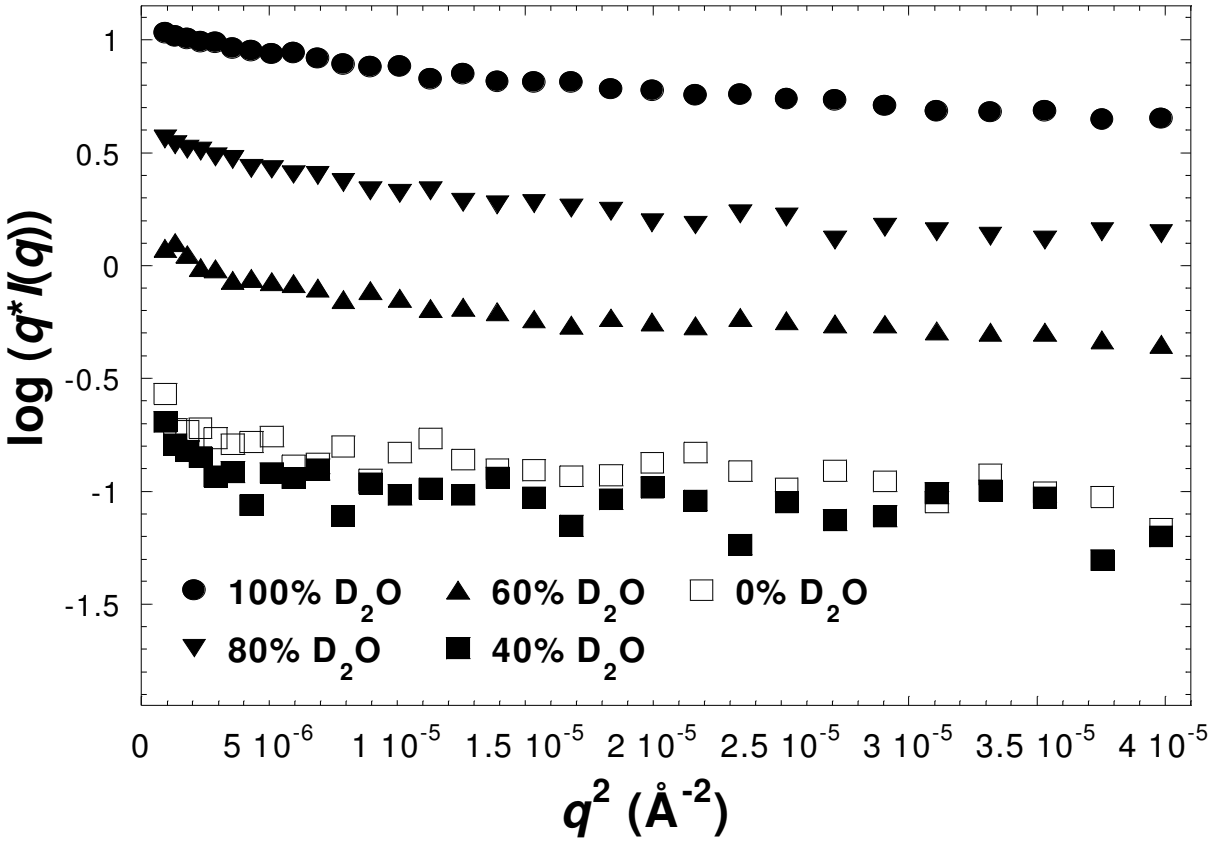

Samples of the chlorosome	R_c (Å, obtained with modified Guinier approximation)
in 100% D_2O	296 ± 6 Å and 196 ± 2 Å
in 80% D_2O	325 ± 10 Å and 160 ± 5 Å
in 60% D_2O	300 ± 10 Å and 140 ± 20 Å
in 40% D_2O	290 ± 40 Å and 190 ± 60 Å
in 25% D_2O	Not determined (low *S*/*N*)
in 0% D_2O	240 ± 50 Å and 220 ± 50 Å

Figure S4. Guinier and modified Guinier approximation for fitting the scattering data of the chlorosome collected in 100% D_2O (20 mM Tris-HCl buffer at pH 8.0). The scattering data (A), the Guinier approximation for the compact particle, $I(q) = I(0)\exp(-q^2R_g^2/3)$ (B), rod (cylinder)-like particle q x $I(q) = I(0)\exp(-q^2R_c^2/2)$ (C), and lamellar (platelet)-like particle, q^2 x $I(q) = I(0)\exp(-q^2R_t^2)$ (D) are shown. Among the Guinier fit, the data can only be fit reasonably by the modified Guinier approximation for rod-like particles (panel C), while $q_{max}*R_g > 1.2$ in the Guinier fit for the compact particles, in addition to no linear region can be used for Guinier fit in the smaller q^2 range (panel B). Further, no Rt can be determined by the modified Guinier fit for the lamellar (platelet)-like particle.

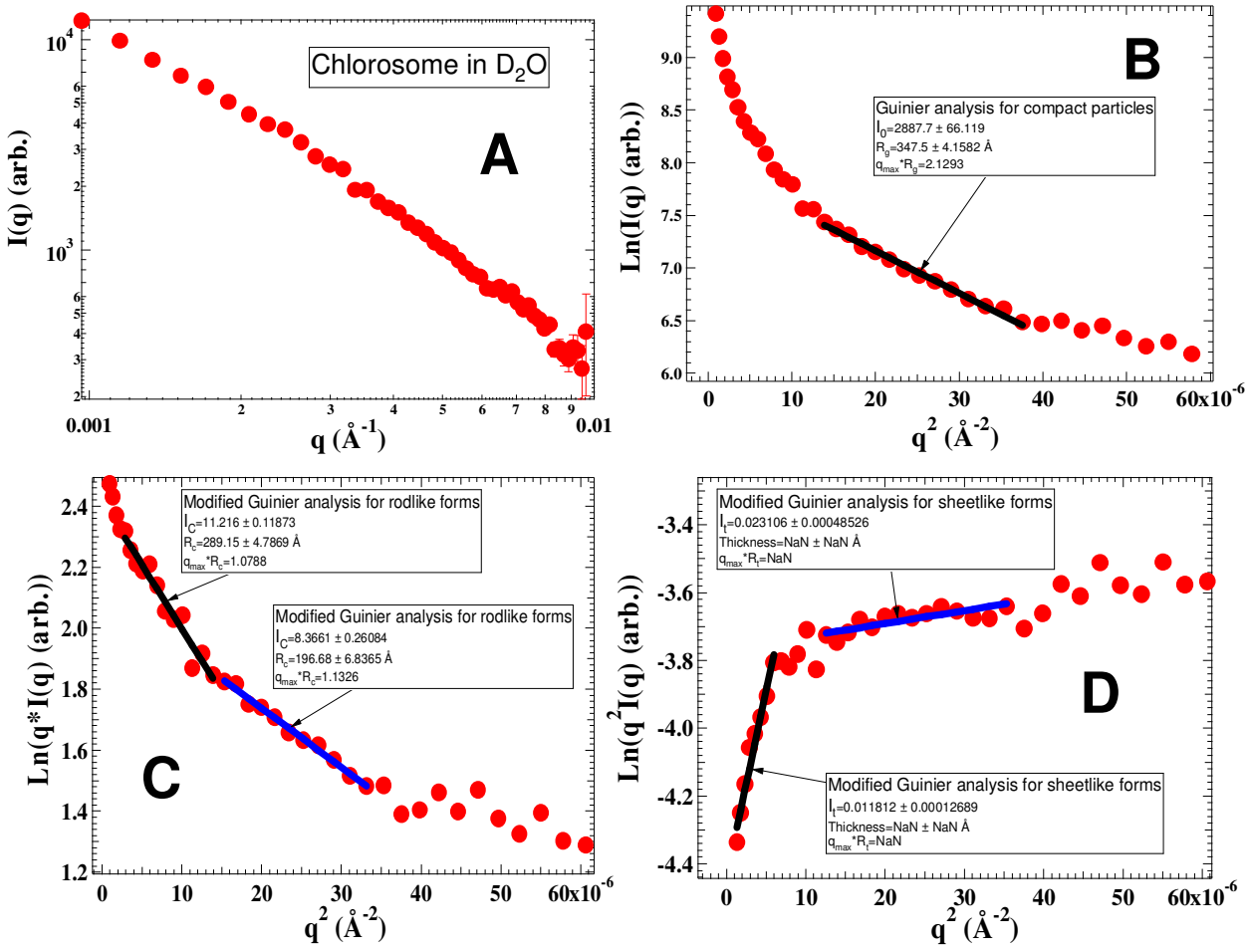

Figure S5. The absorption spectra of the B808-866 complex of *Cfx. aurantiacus* and the LH2 of the purple bacterium *Rps. acidophila*